Available online at www.sciencedirect.com
SCIENCE DIRECT®
Journal of Sound and Vibration 292 (2006) 300–314
JOURNAL OF SOUND AND VIBRATION
www.elsevier.com/locate/jsvi

Free vibrations of clamped–clamped magneto-electro-elastic cylindrical shells

A.R. Annigeri, N. Ganesan, S. Swarnamani*

Machine Design Section, Mechanical Engineering Department, Indian Institute of Technology Madras, Chennai 600 036, India

Received 13 September 2004; received in revised form 14 July 2005; accepted 29 July 2005
Available online 27 September 2005

Abstract

Studies on magneto-electro-elastic cylindrical shell have been carried out in the present work. The constitutive equations of piezomagnetic medium involving mechanical, electrical and magnetic fields are used to derive finite element model for the system. The semi-analytical finite element model is developed. The influence of piezomagnetic effect on the structural frequencies is evaluated. The comparative study of shell with layered configuration with that of multiphase system is attempted. The study is carried out for a typical shell with clamped–clamped boundary conditions.

1. Introduction

Recent literature dealing with research on the behaviour of magneto-electro-elastic structures has gained more importance. Studies on static and dynamic behaviour on plates as well as infinite cylinder has been carried out in literature. Piezoelectric and piezomagnetic composites exhibit coupling effect of electric and magnetic fields. These composite materials can be used as layers or as multiphase. Sunar et al. [1] have studied the finite element modelling of thermopiezomagnetic medium. The behaviour of finitely long cylindrical shells under pressure loading has been studied

*Corresponding author. Tel.: +91 044 2578191; fax: +91 044 2570509.
E-mail address: mani46@iitm.ac.in (S. Swarnamani).

0022-460X/$ - see front matter
doi:10.1016/j.jsv.2005.07.043

by Wang and Zhong [2]. Piezoelectric and piezomagnetic composites in general have the coupling effect which is two order higher than that of constituent materials [2]. Free vibration studies of simply supported and multilayered magneto-electro-elastic plates has been carried out using a propagator matrix approach, reported by Pan and Heyliger [3]. Buchanan [4] has studied the behaviour of infinitely long magneto-electro-elastic cylindrical shells using semi-analytical finite element methods. Recently, Buchanan [5] has studied the behaviour of layered versus multiphase magneto-electro-elastic composites. Pan [6] has derived exact solutions for three dimensional, anisotropic, linearly magneto-electro-elastic, simply supported and multilayered rectangular plates under static loadings. Aboudi [7] has carried out micromechanical analysis of fully coupled electro-magneto-thermo-elastic composites. In his study, a homogenization micromechanical method is employed for the prediction of the effective moduli of magneto-electro-elastic composites. His study includes determination of effective elastic, piezoelectric, piezomagnetic, dielectric, magnetic permeability and electromagnetic coupling moduli, as well as effective thermal expansion coefficients and the associated pyroelectric and pyro-magnetic constants for magneto-electro-elastic composite. Lu et al. [8] have studied frequency behaviour of piezoelectric circular cylindrical shells using an approximate frequency formula. Ng et al. [9] have developed a finite element model for active control of functionally graded shells in frequency domain using piezoelectric sensors and actuators. Ding et al. [10] have conducted a free vibration study of piezoelectric cylindrical shells filled with compressible fluid.

From the literature survey, it is found that only a few studies on magneto-electro-elastic structures have been reported. It is felt that such structures can be used for active vibration control. The study on the vibration behaviour of such structures and influence of piezoelectric and magnetic induction on frequency is extremely useful. Hence in the present study, vibration behaviour of such structures in the form of cylindrical shells is analysed using a semi-analytical finite element approach. $BaTiO_3$ and $CoFe_2O_4$ were used as piezoelectric and piezomagnetic materials, respectively, for the study.

2. Formulation

2.1. Constitutive equations

The coupled constitutive equations for anisotropic and linearly magneto-electro-elastic solids can be written as [3]

$$\sigma_j = C_{jk} S_k - e_{kj} E_k - q_{kj} H_k, \tag{1}$$

$$D_j = e_{jk} S_k + \varepsilon_{jk} E_k + m_{jk} H_k, \tag{2}$$

$$B_j = q_{jk} S_k + m_{jk} E_k + \mu_{jk} H_k, \tag{3}$$

where σ_j denotes stress, D_j is electric displacement and B_j is magnetic induction. C_{jk}, ε_{jk} and μ_{jk} are the elastic, dielectric and magnetic permeability coefficients. e_{kj}, q_{kj} and m_{jk} are piezoelectric, piezomagnetic and magnetoelectric material coefficients. The strain displacement equations for the cylindrical shell are

$$S_{rr} = S_1 = \frac{\partial u}{\partial r}, \quad S_{\theta\theta} = S_2 = \frac{1}{r}\left(\frac{\partial v}{\partial \theta} + u\right), \quad S_{zz} = S_3 = \frac{\partial w}{\partial z},$$

$$S_{\theta z} = S_4 = \frac{\partial v}{\partial z} + \frac{1}{r}\frac{\partial w}{\partial \theta}, \quad S_{rz} = S_5 = \frac{\partial w}{\partial r} + \frac{\partial u}{\partial z}, \quad S_{r\theta} = S_6 = \frac{1}{r}\frac{\partial u}{\partial \theta} + \frac{\partial v}{\partial r} - \frac{v}{r}, \tag{4}$$

where u, v and w are mechanical displacements in coordinate directions r, θ, and z.

The electric field vector E_i is related to the electric potential Φ as shown below:

$$E_r = E_1 = -\frac{\partial \phi}{\partial r}, \quad E_\theta = E_2 = -\frac{1}{r}\frac{\partial \phi}{\partial \theta}, \quad E_z = E_3 = -\frac{\partial \phi}{\partial z}. \tag{5}$$

The magnetic field H_i is related to magnetic potential ψ as shown below:

$$H_r = H_1 = -\frac{\partial \psi}{\partial r}, \quad H_\theta = H_2 = -\frac{1}{r}\frac{\partial \psi}{\partial \theta}, \quad H_z = H_3 = -\frac{\partial \psi}{\partial z}. \tag{6}$$

A completely coupled magneto-electro-elastic material matrix, assuming a hexagonal crystal class, for above constitutive equations can be given below [4].

$$\begin{Bmatrix} \sigma_1 \\ \sigma_2 \\ \sigma_3 \\ \sigma_4 \\ \sigma_5 \\ \sigma_6 \\ D_1 \\ D_2 \\ D_3 \\ B_1 \\ B_2 \\ B_3 \end{Bmatrix} = \begin{bmatrix} C_{11} & C_{12} & C_{13} & 0 & 0 & 0 & 0 & 0 & e_{31} & 0 & 0 & q_{31} \\ C_{12} & C_{11} & C_{13} & 0 & 0 & 0 & 0 & 0 & e_{31} & 0 & 0 & q_{31} \\ C_{13} & C_{13} & C_{33} & 0 & 0 & 0 & 0 & 0 & e_{33} & 0 & 0 & q_{33} \\ 0 & 0 & 0 & C_{44} & 0 & 0 & 0 & e_{15} & 0 & 0 & q_{15} & 0 \\ 0 & 0 & 0 & 0 & C_{44} & 0 & e_{15} & 0 & 0 & q_{15} & 0 & 0 \\ 0 & 0 & 0 & 0 & 0 & C_{66} & 0 & 0 & 0 & 0 & 0 & 0 \\ 0 & 0 & 0 & 0 & e_{15} & 0 & \varepsilon_{11} & 0 & 0 & m_{11} & 0 & 0 \\ 0 & 0 & 0 & e_{15} & 0 & 0 & 0 & \varepsilon_{11} & 0 & 0 & m_{11} & 0 \\ e_{31} & e_{31} & e_{33} & 0 & 0 & 0 & 0 & 0 & \varepsilon_{33} & 0 & 0 & m_{33} \\ 0 & 0 & 0 & 0 & q_{15} & 0 & m_{11} & 0 & 0 & \mu_{11} & 0 & 0 \\ 0 & 0 & 0 & q_{15} & 0 & 0 & 0 & m_{11} & 0 & 0 & \mu_{11} & 0 \\ q_{31} & q_{31} & q_{33} & 0 & 0 & 0 & 0 & 0 & m_{33} & 0 & 0 & \mu_{33} \end{bmatrix} \begin{Bmatrix} S_1 \\ S_2 \\ S_3 \\ S_4 \\ S_5 \\ S_6 \\ E_1 \\ E_2 \\ E_3 \\ H_1 \\ H_2 \\ H_3 \end{Bmatrix}, \tag{7}$$

where $C_{66} = ((C_{11} - C_{12})/2)$.

2.2. Finite element formulation

Semi-analytical finite element approach for the present shell problem is used to express the displacements, electric potential and magnetic potential as trigonometric functions in the circumferential direction as

$$u = \sum u^n \cos n\theta, \quad v = \sum v^n \sin n\theta, \quad w = \sum w^n \cos n\theta,$$

$$\phi = \sum \phi^n \cos n\theta, \quad \psi = \sum \psi^n \cos n\theta. \tag{8}$$

The semi-analytical finite element approach is used to study the magneto-electro-elastic cylindrical shell as the geometry and material properties of the shell does not vary along the θ direction. In such cases, it is possible to consider a series of simplified solutions. Due to the orthogonal property of trigonometric functions, the vibration modes become decoupled and lead to simpler solutions with substantial savings in computational time.

A three noded triangular element is used to model the shell structure with u, v, w, ϕ and ψ as nodal degree of freedom. For clamped–clamped boundary conditions of magneto-electro-elastic shell, $u = v = w = \phi = \psi = 0$, at $z = 0$ and at $z = L$ are assumed. The number of finite elements in the radial direction are 4 and 26 elements along the axial directions were used for the study. The finite element discretization is shown in Fig. 1.

The displacement, electric potential and magnetic potential functions can be generalized in the following form for the nth harmonic:

$$\begin{aligned} u^n &= L_1(u_1 - u_3) + L_2(u_2 - u_3) + u_3, \\ v^n &= L_1(v_1 - v_3) + L_2(v_2 - v_3) + v_3, \\ w^n &= L_1(w_1 - w_3) + L_2(w_2 - w_3) + w_3, \\ \phi^n &= L_1(\phi_1 - \phi_3) + L_2(\phi_2 - \phi_3) + \phi_3, \\ \psi^n &= L_1(\psi_1 - \psi_3) + L_2(\psi_2 - \psi_3) + \psi_3. \end{aligned} \tag{9}$$

After integrating in θ direction, a formulation for such coupled field can be written as [2]

$$\begin{aligned} [[K_{uu}] - \omega^2[M]]\{U\} + [K_{u\phi}]\{\phi\} + [K_{u\psi}]\{\psi\} &= 0, \\ [K_{u\phi}]^{\mathrm{T}}\{U\} - [K_{\phi\phi}]\{\phi\} - [K_{\phi\psi}]\{\psi\} &= 0, \\ [K_{u\psi}]^{\mathrm{T}}\{U\} - [K_{\phi\psi}]^{\mathrm{T}}\{\phi\} - [K_{\psi\psi}]\{\psi\} &= 0. \end{aligned} \tag{10}$$

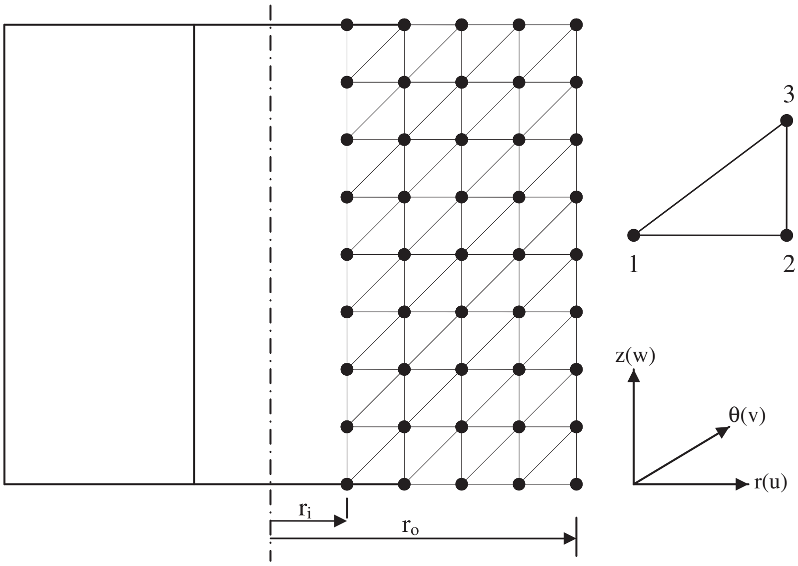

Fig. 1. Shell discretization for three noded triangular elements.

Various stiffness matrices are defined as shown below:

$$[K_{uu}] = c\int_v [B_u]^{\mathrm{T}}[C][B_u]\,\mathrm{d}A,$$

$$[K_{u\phi}] = c\int_v [B_u]^{\mathrm{T}}[e][B_\phi]\,\mathrm{d}A,$$

$$[K_{u\psi}] = c\int_v [B_u]^{\mathrm{T}}[q][B_\psi]\,\mathrm{d}A,$$

$$[K_{\phi\phi}] = c\int_v [B_\phi]^{\mathrm{T}}[\varepsilon][B_\phi]\,\mathrm{d}A,$$

$$[K_{\psi\psi}] = c\int_v [B_\psi]^{\mathrm{T}}[\mu][B_\psi]\,\mathrm{d}A,$$

$$[K_{\phi\psi}] = c\int_v [B_\phi]^{\mathrm{T}}[m][B_\psi]\,\mathrm{d}A,$$

$$[M] = c\int_v [N]^{\mathrm{T}}[\rho][N]\,\mathrm{d}A, \tag{11}$$

where $[B_u]$, $[B_\phi]$ and $[B_\psi]$ are for strain–displacement, electric field–electric potential and magnetic field–magnetic potential, respectively, where $\mathrm{d}A = 2\pi r\,\mathrm{d}r\,\mathrm{d}z$ and

$$c = 2\pi \quad \text{for } n = 0,$$

$$c = 1 \quad \text{for } n > 0.$$

In Eq. (10), elimination of electric and magnetic potential was done by condensation techniques to get $[K_{\mathrm{eq}}]$.

$$[K_{\mathrm{eq}}]\{U\} + [M]\{\ddot{U}\} = 0, \tag{12}$$

where

$$[K_{\mathrm{eq}}] = [K_{uu}] + [K_{u\phi}][K_{\mathrm{II}}]^{-1}[K_{\mathrm{I}}] + [K_{u\psi}][K_{\mathrm{V}}]^{-1}[K_{\mathrm{IV}}]. \tag{13}$$

The component matrices for Eq. (13) are

$$[K_{\mathrm{I}}] = [K_{u\phi}]^{\mathrm{T}} - [K_{\phi\psi}][K_{\psi\psi}]^{-1}[K_{u\psi}]^{\mathrm{T}}, \tag{14}$$

$$[K_{\mathrm{II}}] = [K_{\phi\phi}] - [K_{\phi\psi}][K_{\psi\psi}]^{-1}[K_{\phi\psi}]^{\mathrm{T}}, \tag{15}$$

$$[K_{\mathrm{IV}}] = [K_{u\psi}]^{\mathrm{T}} - [K_{\phi\psi}]^{\mathrm{T}}[K_{\phi\phi}]^{-1}[K_{u\phi}]^{\mathrm{T}}, \tag{16}$$

$$[K_{\mathrm{V}}] = [K_{\psi\psi}] - [K_{\phi\psi}]^{\mathrm{T}}[K_{\phi\phi}]^{-1}[K_{\phi\psi}]. \tag{17}$$

The eigenvectors that correspond to the distribution of $\{\phi\}$ and $\{\psi\}$ can be as shown below.

$$\phi = [K_{\mathrm{II}}]^{-1}[K_{\mathrm{I}}]\{U\}, \tag{18}$$

$$\psi = [K_{\mathrm{V}}]^{-1}[K_{\mathrm{IV}}]\{U\}. \tag{19}$$

Table 1
List of stiffness matrices used in the study

Symbol	Meaning
$[K_{uu}]$	Structural stiffness matrix considering elastic constants
$[K_{eq}]$	System stiffness matrix with magneto-electro-elastic material properties
$[K_{eq\_reduced}]$	System stiffness matrix neglecting magnetoelectric coupling
$[K_{eq\_\phi\phi}]$	System stiffness matrix considering piezoelectric effect
$[K_{eq\_\psi\psi}]$	System stiffness matrix considering piezomagnetic effect

The equivalent stiffness matrix $[K_{eq\_reduced}]$ is derived by neglecting the coupling between piezoelectric $BaTiO_3$ and piezomagnetic $CoFe_2O_4$ materials. The magnetoelectric material coefficient (m) is zero for single phase $BaTiO_3$ and $CoFe_2O_4$ [4].

From Eq. (10), the reduced equations are

$$[[K_{uu}] - \omega^2[M]]\{U\} + [K_{u\phi}]\{\phi\} + [K_{u\psi}]\{\psi\} = 0,$$

$$[K_{u\phi}]^{T}\{U\} - [K_{\phi\phi}]\{\phi\} = 0,$$

$$[K_{u\psi}]^{T}\{U\} - [K_{\psi\psi}]\{\psi\} = 0. \tag{20}$$

Using a static condensation method to eliminate $\{\phi\}$ and $\{\psi\}$, the relation for $[K_{eq\_reduced}]$ is given below.

$$[K_{eq\_reduced}] = [K_{uu}] + [K_{u\phi}][K_{\phi\phi}]^{-1}[K_{u\phi}]^{T} + [K_{u\psi}][K_{\psi\psi}]^{-1}[K_{u\psi}]^{T}. \tag{21}$$

To study the piezoelectric effect on frequency due to $BaTiO_3$ material, the stiffness matrix $[K_{eq\_\phi\phi}]$ is derived and is given by

$$[K_{eq\_\phi\phi}] = [K_{uu}] + [K_{u\phi}][K_{\phi\phi}]^{-1}[K_{u\phi}]^{T}. \tag{22}$$

To study the magnetic effect on frequency due to magnetic $CoFe_2O_4$ material $[K_{eq\_\psi\psi}]$ is used as the stiffness matrix and is shown below:

$$[K_{eq\_\psi\psi}] = [K_{uu}] + [K_{u\psi}][K_{\psi\psi}]^{-1}[K_{u\psi}]^{T}. \tag{23}$$

Table 1 gives the list of the stiffness matrices used in the study of the magneto-electro-elastic shell.

3. Results and discussion

3.1. Validation

The validation is done using the series solution method reported by Annigeri et al. [11] for an finite magneto-electro-elastic solid shell with simply supported boundary conditions. The results are shown in Table 2. The dimensions of the magneto-electro-elastic shell are: length = 4 m, inner radius = 0.7 m, outer radius = 1.3 m. The results of the present formulation match well for all circumferential harmonics.

Table 2
Comparison for different circumferential harmonics for first axial mode

n	$f_{K_{uu}}$ (Hz)	$f_{K_{eq}}$ (Hz)	$f_{K_{eq\_reduced}}$ (Hz)	$f_{K_{eq\_\psi\psi}}$ (Hz)	$f_{K_{eq\_\phi\phi}}$ (Hz)
(a) Using triangular elements, for vf = 100% for simply supported boundary conditions, i.e., $w=\phi=\psi=0$ at $z=0$ and L of the shell					
1	202.4	209.7	209.7	202.4	209.7
2	349.5	352.7	352.7	349.5	352.7
3	766.2	767.8	767.8	766.2	767.8
4	1226.0	1228.0	1228.0	1226.0	1228.0
5	1690.0	1691.0	1691.0	1690.0	1691.0
(b) With series solution for series solution with $w=\phi=\psi=0$ at $z=0$ and l of the shell					
1	201.8	202.4	202.4	201.8	202.4
2	349.3	349.6	349.7	349.3	349.6
3	759.4	760.2	760.2	759.4	760.2
4	1209.8	1210.8	1210.8	1209.8	1210.8
5	1661.8	1662.9	1662.9	1661.8	1662.9

3.2. Frequency studies on $BaTiO_3$ and $CoFe_2O_4$ cylindrical shells

In order to understand the behaviour of piezoelectric $BaTiO_3$ and piezomagnetic $CoFe_2O_4$ materials frequency analysis of a shell with inner radius $(r_i) = 0.7$ m, outer radius $(r_o) = 1.3$ m, length $(L) = 4.0$ m, r/t ratio = 1.66, L/r ratio = 4 is carried out. The material properties are given in Table 3 and the values are obtained from the graphical results of Aboudi [7] and for simplicity, the density for both $BaTiO_3$ and $CoFe_2O_4$ is assumed to be 5730 kg/m^3 [3]. A typical multiphase shell is shown in Fig. 2. To understand the influence of piezoelectric and piezomagnetic effects on shell frequencies, different stiffness matrices $[K_{uu}]$, $[K_{eq}]$, $[K_{eq\_reduced}]$, $[K_{eq\_\phi\phi}]$ and $[K_{eq\_\psi\psi}]$ are used along with the conventional mass matrix to evaluate the frequencies of the system. The parameter λ representing normalized squared structural frequency is computed as

$$\lambda_{[K_{eq}]} = \frac{\text{Eigenvalue caused by } [K_{eq}]}{\text{Eigenvalue caused by } [K_{uu}]},$$

$$\lambda_{[K_{eq\_reduced}]} = \frac{\text{Eigenvalue caused by } [K_{eq\_reduced}]}{\text{Eigenvalue caused by } [K_{uu}]},$$

$$\lambda_{[K_{eq\_\psi\psi}]} = \frac{\text{Eigenvalue caused by } [K_{eq\_\psi\psi}]}{\text{Eigenvalue caused by } [K_{uu}]},$$

$$\lambda_{[K_{eq\_\phi\phi}]} = \frac{\text{Eigenvalue caused by } [K_{eq\_\phi\phi}]}{\text{Eigenvalue caused by } [K_{uu}]}.$$

Table 4 shows the frequency (in Hz) for the first seven harmonic values for vf = 100% of $BaTiO_3$ in $BaTiO_3$–$CoFe_2O_4$ composite. The data corresponds to structural frequency of the shell $f_{K_{uu}}$, system frequency of the shell $f_{K_{eq}}$, system frequency by neglecting magnetoelectric coupling

Table 3
Material constants as a percentage (volume fraction vf) of $BaTiO_3$ in $BaTiO_3$–$CoFe_2O_4$ composite [7]

vf	0.0	0.2	0.4	0.6	0.8	1.0
C_{11}	286	250	225	200	175	166
C_{12}	173	146	125	110	100	77
C_{13}	170	145	125	110	100	78
C_{33}	269.5	240	220	190	170	162
C_{44}	45.3	45	45	45	50	43
e_{15}	0	0	0	0	0	11.6
e_{31}	0	−2	−3	−3.5	−4	−4.4
e_{33}	0	4	7	11	14	18.6
ε_{31}	0.08	0.33	0.8	0.9	1.0	11.2
ε_{33}	0.093	2.5	5.0	7.5	10	12.6
μ_{11}	−5.9	−3.9	−2.5	−1.5	−0.8	0.05
μ_{33}	1.57	1.33	1.0	0.75	0.5	0.1
q_{15}	560	340	220	180	80	0
q_{31}	580	410	300	200	100	0
q_{33}	700	550	380	260	120	0
m_{11}	0	2.8	4.8	6.0	6.8	0
m_{33}	0	2000	2750	2500	1500	0

C_{ij} in $10^9\,N/m^2$, e_{ij} in C/m^2, ε_{ij} in $10^{-9}\,C/V\,m$, q_{ij} in $N/A\,m$, μ_{ij} in $10^{-4}\,N\,s^2/C^2$ and m_{ij} in $10^{-12}\,N\,s/VC$.

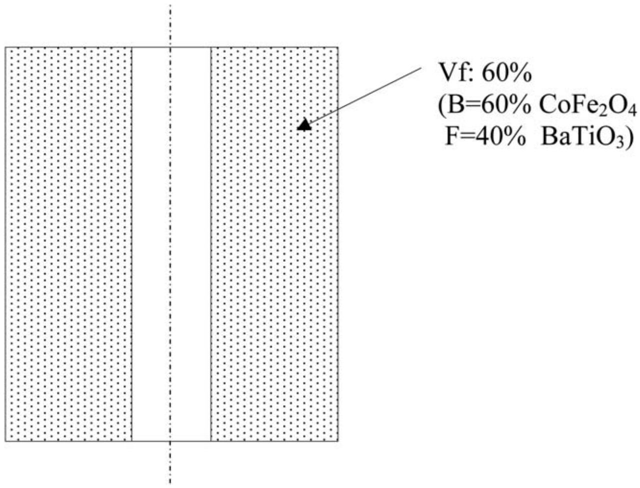

Fig. 2. Single layered multiphase cylindrical shell.

$f_{K_{eq\_reduced}}$, system frequency of the shell considering piezoelectric effect $f_{K_{eq\_\psi\psi}}$, system frequency of the shell considering piezomagnetic effect $f_{K_{eq\_\phi\phi}}$.

Fig. 3 shows the plot of eigenvalues normalized by structural eigenvalues for cylindrical shell made of piezoelectric $BaTiO_3$ (vf = 100% $BaTiO_3$ in $BaTiO_3$–$CoFe_2O_4$ composite). The graph

Table 4
Frequencies (in Hz) for vf = 100% $BaTiO_3$ in $BaTiO_3$–$CoFe_2O_4$ composite

n	$f_{K_{uu}}$ (Hz)	$f_{K_{eq}}$ (Hz)	$f_{K_{eq\_reduced}}$ (Hz)	$f_{K_{eq\_\psi\psi}}$ (Hz)	$f_{K_{eq\_\phi\phi}}$ (Hz)
0	559.47	613.85	613.85	559.47	613.85
1	268.60	272.39	272.39	268.60	272.39
2	397.87	409.19	409.19	397.87	409.19
3	789.60	801.06	801.06	789.60	801.06
4	1241.25	1253.23	1253.23	1241.25	1253.23
5	1700.58	1713.93	1713.93	1700.58	1713.93
6	2149.79	2165.05	2165.05	2149.79	2165.05

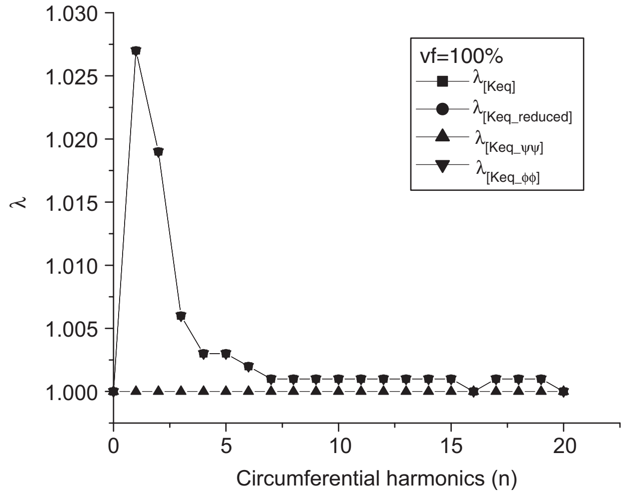

Fig. 3. Effect of normalized structural eigenvalues for first axial mode for $BaTiO_3$ vf = 100%.

shows predominantly two curves for the first 20 circumferential modes for first axial mode. The parameter $\lambda_{[K_{eq\_\psi\psi}]}$ shows constant values of unity for first 20 circumferential harmonics, indicating structural eigenvalue due to K_{uu} and eigenvalue due to $K_{eq\_\psi\psi}$ being same. This is due to the fact that the shell is made of only piezomagnetic material and there is no coupling effect between piezoelectric and magnetoelectric components. Hence the eigenvalues due to K_{eq}, $K_{eq\_reduced}$ and $K_{eq\_\phi\phi}$ are equal depicting two graphs in the figure. Also for first five modes, the eigenvalues due to K_{eq}, $K_{eq\_reduced}$ and $K_{eq\_\phi\phi}$ show higher values than unity, but for higher harmonics ($n>6$), the eigenvalues due to K_{eq}, becomes equal to eigenvalue due to K_{uu}.

Fig. 4 shows the eigenvalues normalized by structural eigenvalues for cylindrical shell made of piezomagnetic $CoFe_2O_4$ (vf = 0% $BaTiO_3$ in $BaTiO_3$–$CoFe_2O_4$ composite). The graph shows predominantly two curves for the first 20 circumferential modes for first axial modes. The parameter $\lambda_{[K_{eq\_\phi\phi}]}$ shows constant value of unity for first 20 circumferential harmonics, indicating

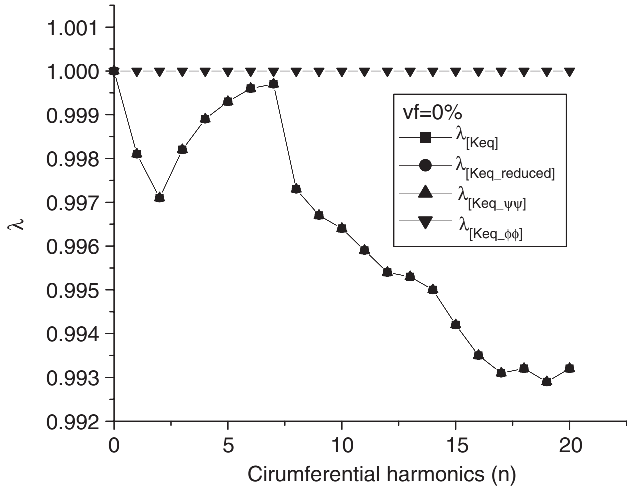

Fig. 4. Effect of normalized structural eigenvalues for first axial mode for $BaTiO_3$ vf = 0%.

Table 5
Frequencies (in Hz) for vf = 0% $BaTiO_3$ in $BaTiO_3$–$CoFe_2O_4$ composite

n	$f_{K_{uu}}$ (Hz)	$f_{K_{eq}}$ (Hz)	$f_{K_{eq\_reduced}}$ (Hz)	$f_{K_{eq\_\psi\psi}}$ (Hz)	$f_{K_{eq\_\phi\phi}}$ (Hz)
0	635.94	634.54	634.54	634.54	635.94
1	284.67	284.40	284.40	284.40	284.67
2	455.61	451.42	451.42	451.42	455.61
3	914.43	905.81	905.81	905.81	914.43
4	1432.47	1416.65	1416.65	1416.65	1432.47
5	1954.18	1923.49	1923.49	1923.49	1954.18
6	2461.70	2379.58	2379.58	2379.58	2461.70

structural eigenvalue due to K_{uu} and eigenvalue due to $K_{eq\_\phi\phi}$ being same. This is due to the fact that the shell is made of only piezomagnetic material and there is no piezoelectric and no magnetoelectric coupling effect. Hence the eigenvalues due to K_{eq}, $K_{eq\_reduced}$ and $K_{eq\_\phi\phi}$ are equal depicting two graphs in the figure. Table 5 shows the frequency (in Hz) for the first seven harmonic values for vf = 0% of $BaTiO_3$ in $BaTiO_3$–$CoFe_2O_4$ composite.

3.2.1. Frequency behaviour of composite shells

Fig. 5 shows a composite shell with the stacking sequence B/F. Here, the inner shell is made of 100% $BaTiO_3$ material (B) and outer shell is made of 100% $CoFe_2O_3$ material (F).

Fig. 6 shows eigenvalues for a composite shell with the stacking sequence (B/F) as inner shell is of $BaTiO_3$ material (B) and outer shell is made of $CoFe_2O_3$ material (F). The parameters $\lambda_{[K_{eq}]}$, $\lambda_{[K_{eq\_\phi\phi}]}$ and $\lambda_{[K_{eq\_\psi\psi}]}$ are clearly visible in the figure. The piezoelectric and piezomagnetic effect on the system frequency is observed upto $n = 5$. After 5th circumferential harmonics, the effect of piezoelectric and piezomagnetic is not predominant.

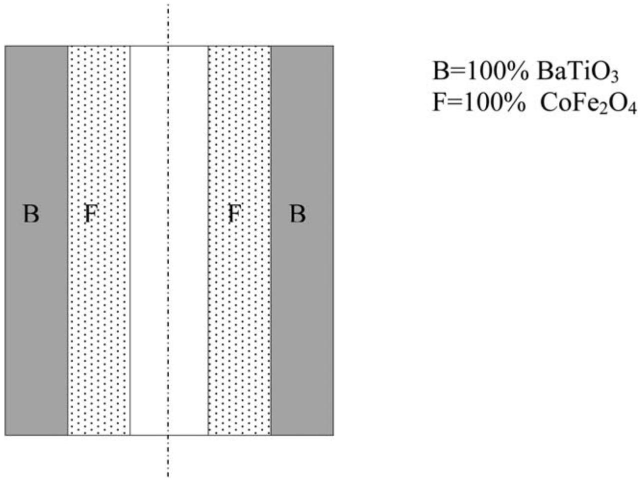

Fig. 5. Two layered cylindrical shell for B/F stacking.

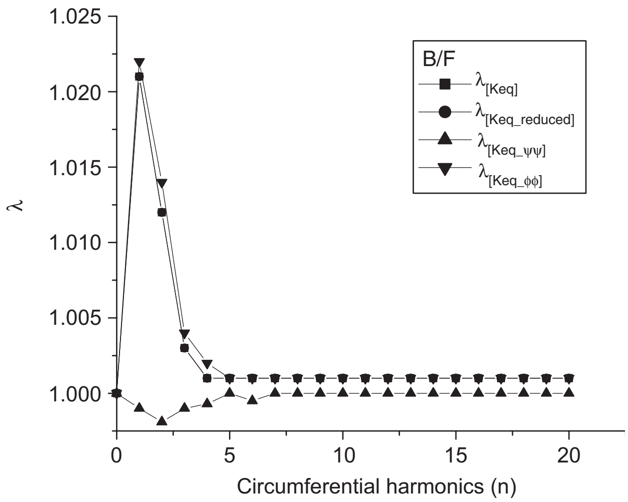

Fig. 6. Effect of normalized structural eigenvalues for first axial mode for composite shells (B/F stacking).

Fig. 7 shows the results of eigenvalues for F/B stacking of shells, i.e., inner shell is of $CoFe_2O_3$ material and outer shell is made of $BaTiO_3$ material. For initial two modes, due to higher magnetic effect, the eigenvalue due to $K_{eq\_\psi\psi}$ is less than the eigenvalue due to K_{uu}. It can be observed that the influence of piezoelectric effect is to increase the frequency of the system and the magnetic effect is to reduce the frequency of the system. Also it is noticed here that after the 9th mode, the eigenvalue slightly decreases. It may be due to increased magnetic effect.

It is observed from these figures, that the effect of $BaTiO_3$ shell is to increase the frequency due to piezoelectric effect and the magnetic effect due to $CoFe_2O_4$ is to reduce the frequency of the system.

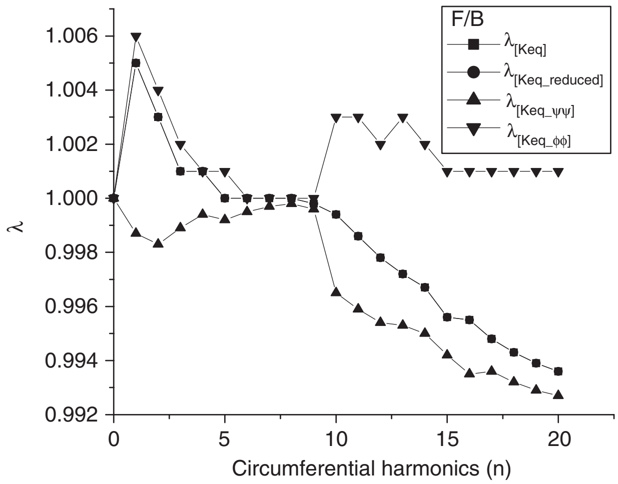

Fig. 7. Effect of normalized structural eigenvalues for first axial mode for composite shell (*F*/*B* stacking).

3.2.2. Frequency behaviour of multiphase shells

In order to understand the behaviour of the non-dimensional frequency on different shells for vf $=0.2$–0.8 is shown in Figs. 8–11. Fig. 8 shows the graphs of eigenvalues normalized by structural eigenvalues for cylindrical shell made of 20% $BaTiO_3$ in $BaTiO_3$–$CoFe_2O_4$ composite. The graph shows predominantly three curves for the first 20 circumferential modes for first axial modes. The parameters $\lambda_{[K_{eq}]}$, $\lambda_{[K_{eq\_reduced}]}$, $\lambda_{[K_{eq\_\phi\phi}]}$ show higher values than unity, indicating higher eigenvalues for the first 6 circumferential harmonics. For this shell the piezomagnetic effect reduces the system frequency. This can be observed from the $\lambda_{[K_{eq\_\psi\psi}]}$ graph is less than unity for first six harmonics and it brings down the system frequency, but for higher harmonics the eigenvalues due to K_{eq}, becomes slightly less than the eigenvalue due to K_{uu}.

Fig. 9 shows the plot of vf $=40\%$ the similar trend as observed in Fig. 13 for vf $=20\%$, for first few modes the parameters $\lambda_{[K_{eq}]}$, $\lambda_{[K_{eq\_reduced}]}$, $\lambda_{[K_{eq\_\phi\phi}]}$ are more than unity and become equal to eigenvalue due to K_{uu}. At higher modes, the piezoelectric and piezomagnetic effects on the system frequency are not felt.

Fig. 10 shows the plot for vf $=60\%$, the trend is similar to the earlier graphs with eigenvalues due to K_{uu} and K_{eq} becoming equal at higher modes. Here the magnetic effect is less as the shell is composed of 40% $CoFe_2O_4$ and 60% $BaTiO_3$ in $BaTiO_3$–$CoFe_2O_4$ composite.

Fig. 11, for vf $=80\%$ show the trend in which the eigenvalue due to $K_{eq\_\psi\psi}$ is more than unity for first few modes. It is due to the fact that the composition of the shell is 20% $CoFe_2O_4$ and 80% $BaTiO_3$ in $BaTiO_3$–$CoFe_2O_4$ composite. For higher modes, the system the eigenvalue becomes almost equal to eigenvalue due to K_{uu}.

In all the above studies, the magnetoelectric coupling effect is not felt and it can be observed from the above figures that plots of $\lambda_{[K_{eq}]}$ and $\lambda_{[K_{eq\_reduced}]}$ merge at all circumferential modes.

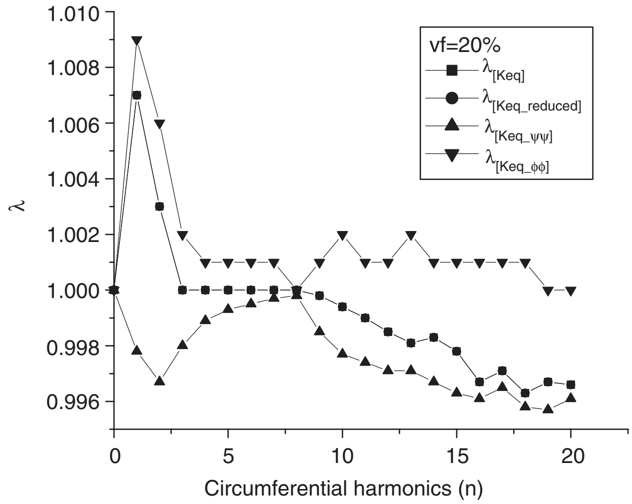

Fig. 8. Effect of normalized structural eigenvalues for first axial mode for $BaTiO_3$ vf $= 20\%$.

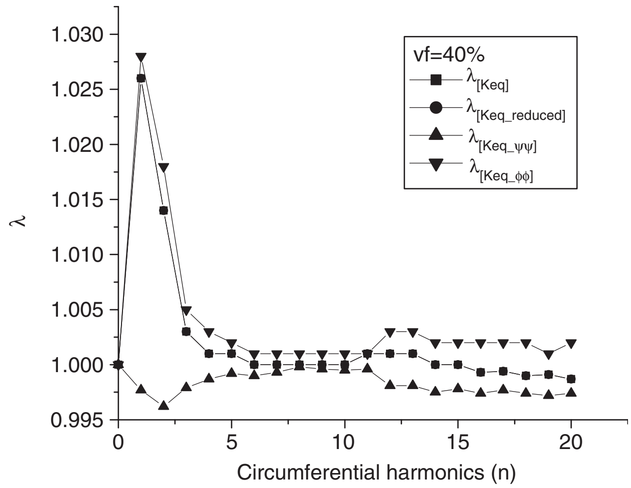

Fig. 9. Effect of normalized structural eigenvalues for first axial mode for $BaTiO_3$ vf $= 40\%$.

4. Conclusion

In the present study, the frequency behaviour of clamped–clamped magneto-electro-elastic cylindrical shells were analysed using the semi-analytical finite element approach. The influence of piezoelectric and magnetic effect on the system frequencies as well as coupling between piezoelectric and piezomagnetic effect were also analysed. Based on the study:

(1) In general, the piezoelectric effect has the tendency of stiffening the shell and hence increases the natural frequency.

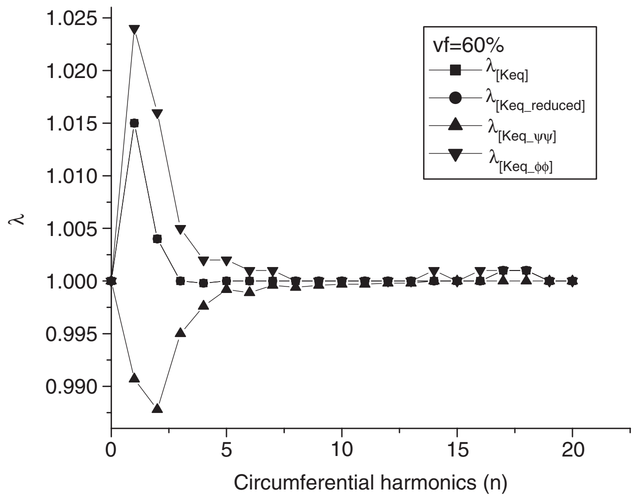

Fig. 10. Effect of normalized structural eigenvalues for first axial mode for $BaTiO_3$ vf = 60%.

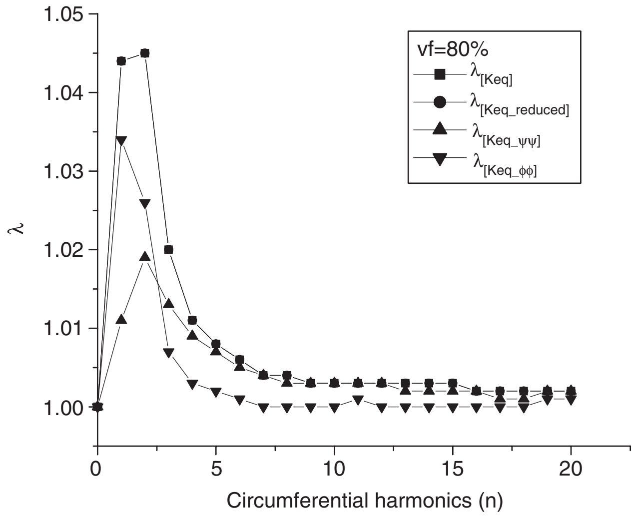

Fig. 11. Effect of normalized structural eigenvalues for first axial mode for $BaTiO_3$ vf = 80%.

(2) The magnetic effect is to reduce the stiffness of system and bring down the frequency of the system; in case of composite shells, the total effect is to increase the natural frequency of the system, depending on the composition.
(3) In case of multiphase shells, the volume fraction (vf) of $BaTiO_3$ in $BaTiO_3$–$CoFe_2O_4$ composite has considerable effect on the frequency of the system.
(4) The above-mentioned effects are predominant at lower circumferential modes and at higher circumferential modes, the piezoelectric and piezomagnetic effect is negligible.

Acknowledgements

The authors would like to thank Prof. G.R. Buchanan, Department of Civil and Environmental Engineering, Tennessee Technological University, Cookeville, TN 38506, USA, for his valuable suggestions and clarifications at various stages of the study.

References

[1] M. Sunar, A.Z. Al-Garni, M.H. Ali, R. Kahraman, Finite element modeling of thermopiezomagnetic smart structures, *AIAA Journal* 40 (2002) 1846–1851.
[2] X. Wang, Z. Zhong, A finitely long circular cylindrical shell of piezoelectric/piezomagnetic composite under pressuring and temperature change, *International Journal of Engineering Science* 41 (2003) 2429–2445.
[3] E. Pan, P.R. Heyliger, Free vibrations of simply supported and multilayered magneto-electro-elastic plates, *Journal of Sound and Vibration* 252 (2002) 429–442.
[4] G.R. Buchanan, Free vibration of an infinite magneto-electro-elastic cylinder, *Journal of Sound and Vibration* 268 (2003) 413–426.
[5] G.R. Buchanan, Layered versus multiphase magneto-electro-elastic composites, *Composites Part B* 35 (2004) 413–420.
[6] E. Pan, Exact solution for simply supported and multilayered magneto-electro-elastic plates, *Transactions of the ASME* 68 (2001) 608–618.
[7] J. Aboudi, Micromechanical analysis of fully coupled electro-magneto-thermo-elastic multiphase composites, *Smart Materials and Structures* 10 (2001) 867–877.
[8] P. Lu, K.H. Lee, W.Z. Lin, F. Shen, S.P. Lim, An approximate frequency formula for piezoelectric circular cylindrical shells, *Journal of Sound and Vibration* 242 (2001) 309–320.
[9] T.Y. Ng, X.Q. He, K.M. Liew, Finite element modeling of active control of functionally graded shells in frequency domain via piezoelectric sensors and actuators, *Computational Mechanics* 28 (2002) 1–9.
[10] H.J. Ding, W.Q. Chen, Y.M. Guo, Q.D. Yang, Free vibration of piezoelectric cylindrical shells filled with compressible fluid, *International Journal of Solids and Structures* 34 (1997) 2025–2034.
[11] A.R. Annigeri, N. Ganesan, S. Swarnamani, Free vibration studies of simply supported layered and multiphase magneto-electro-elastic cylindrical shells, *Smart Materials and Structures* (communicated).